Journal of Power Sources 279 (2015) 737–744

Contents lists available at ScienceDirect

Journal of Power Sources

journal homepage: www.elsevier.com/locate/jpowsour

Surface-modified separators prepared with conductive polymer and aluminum fluoride for lithium-ion batteries

Won-Kyung Shin, Ji-Hyun Yoo, Dong-Won Kim*

Department of Chemical Engineering, Hanyang University, Seungdong-Gu, Seoul 133-791, Republic of Korea

HIGHLIGHTS

- Polyethylene separators are surface-modified by coating with conductive polymer and aluminum fluoride particles.
- The surface-modified separators exhibit a significant reduction in thermal shrinkage and an improved electrolyte uptake.
- Lithium-ion cells with surface-modified separators exhibit better cycling performance than a cell with a pristine separator.

ARTICLE INFO

Article history:
Received 5 November 2014
Received in revised form
17 December 2014
Accepted 8 January 2015
Available online 10 January 2015

Keywords:
Surface-modified separators
Conductive polymer
Aluminum fluoride
Lithium-ion cells
Thermal stability

ABSTRACT

Conventional polyethylene (PE) separators are surface-modified by thin coating with conductive poly(3,4-ethylenedioxythiophen)-*co*-poly(ethylene glycol) (PEDOT-*co*-PEG) copolymer and aluminum fluoride particles. The surface-modified separators exhibit a significant reduction in thermal shrinkage and an improved electrolyte uptake. By using these separators, the lithium-ion cells composed of carbon negative electrodes and $LiNi_{1/3}Co_{1/3}Mn_{1/3}O_2$ positive electrodes are assembled and their cycling performances are evaluated. The cells assembled with the surface-modified separators demonstrate superior cycling performance compared to cells prepared with pristine PE separator, both at ambient temperatures and at elevated temperature.

© 2015 Elsevier B.V. All rights reserved.

1. Introduction

The demand for rechargeable lithium-ion batteries for application in portable electronic devices, electric vehicles and energy storage systems has rapidly increased [1–4]. In the lithium-ion battery, a separator is a critical component that affects both cycling performance and safety, while permitting fast Li^+ ion transport in the cell. Polyolefins separators such as polyethylene (PE) and polypropylene have been widely used in lithium-ion batteries because of their low cost, excellent mechanical strength and chemical stability [5,6]. However, they may shrink, soften and even melt at elevated temperatures, causing short circuits between two electrodes in cases where unusually high heat is generated [7–9]. Furthermore, their hydrophobic nature leads pores in the separator to be not completely filled with liquid electrolyte due to poor wettability for polar organic electrolytes, which results in high ionic resistance [10,11]. To solve these problems, extensive studies have been carried out on techniques to coat the surface of polyolefin separators with organic and inorganic materials [12–16]. Although such coatings have been effective in improving the mechanical, thermal and electrical properties of polyolefin separators, the addition of a coating layer a few micrometers thick decreases the energy density and high power capability of the batteries. It is thus highly desirable to reduce the thickness of the coating layers on the separators, while enhancing their thermal, mechanical and electrochemical properties. In our previous studies, a thin polymer layer based on poly(3,4-ethylenedioxythiophene)-*co*-poly(ethylene glycol) (PEDOT-*co*-PEG) copolymer was coated onto lithium electrodes or $LiNi_{0.6}Co_{0.2}Mn_{0.2}O_2$ active materials to improve their electrochemical performance [17,18]. This copolymer is a highly ion-conductive polymer that transports lithium ions and has strong adhesive properties that allow it to form a stable thin layer on the substrate. These results prompted us to use PEDOT-*co*-PEG copolymer as a thin coating material on PE separator. As an inorganic coating material, we employed aluminum fluoride (AlF_3), because it

* Corresponding author.
E-mail address: dongwonkim@hanyang.ac.kr (D.-W. Kim).

http://dx.doi.org/10.1016/j.jpowsour.2015.01.047
0378-7753/© 2015 Elsevier B.V. All rights reserved.

has been reported that the use of aluminum fluoride in the electrolyte or on electrode materials could improve thermal stability and electrochemical performance by suppressing electrolyte decomposition [19–23].

With the goal of developing thin separators with high thermal stability and good electrochemical properties, we modified the surface of PE separator with PEDOT-*co*-PEG copolymer and AlF_3 particles. Due to the thinness of the coating layer, its addition to the separator does not deteriorate the cell's energy density or high rate capability. Using these surface-modified separators, we assembled lithium-ion cells based on carbon negative electrodes and $LiNi_{1/3}Co_{1/3}Mn_{1/3}O_2$ positive electrodes. The cycling performance of cells assembled with surface-modified separators was evaluated and compared to that of cell with a pristine PE separator. Surface modification of the PE separator with the PEDOT-*co*-PEG and AlF_3 was demonstrated to be very effective in improving thermal stability, cycling stability and high rate performance.

2. Experimental

2.1. Surface modification of PE separator

PEDOT-*co*-PEG solution (Sigma–Aldrich) was used as received. Aluminum fluoride (Sigma–Aldrich) was dispersed into the solution at a concentration of 10 wt% based on the weight of the PEDOT-*co*-PEG copolymer. The particle size of aluminum fluoride was less than 20 nm. When the mixture was completely homogenized, the resulting solution was applied to both sides of a PE separator (SK Innovation Co.) that was 9 μm thick and of 40% porosity. Next, the coated separator was dried at room temperature for 30 min to allow the solvent to evaporate, followed by additional drying in a vacuum oven at 80 °C for 24 h. The coating thickness was adjusted by changing the content of the PEDOT-*co*-PEG copolymer and AlF_3 in the solution to obtain surface-modified separator with a thickness of 10 μm.

2.2. Electrode preparation and cell assembly

The positive electrode was prepared by coating an N-methyl pyrrolidine (NMP)-based slurry containing 85.0 wt% $LiNi_{1/3}Co_{1/3}Mn_{1/3}O_2$ (3M Co.), 7.5 wt% poly(vinylidene fluoride) (PVdF) and 7.5 wt% super-P carbon (MMM Co.) onto an aluminum foil. Its active mass loading corresponded to a capacity of about 2.0 mAh cm^{-2}. The negative electrode was prepared similarly by coating an NMP-based slurry of mesocarbon microbeads (MCMB, Osaka gas), PVdF and super-P carbon (88:8:4 by weight) onto a copper foil. Lithium-ion cell was assembled by sandwiching a surface-modified separator between the carbon negative electrode and the $LiNi_{1/3}Co_{1/3}Mn_{1/3}O_2$ positive electrode. The cell was then enclosed in a 2032 coin cell and injected with electrolyte solution, which consisted of 1.15 M $LiPF_6$ in 3:5:2 (by volume) mixture of ethylene carbonate (EC), ethylmethyl carbonate (EMC) and diethyl carbonate (DEC) containing 5 wt% fluoroethylene carbonate (FEC) (battery grade, Soulbrain Co. Ltd.). All cells were assembled in a dry box filled with argon gas.

2.3. Measurements

The morphologies of separators were examined using a field emission scanning electron microscope (FE-SEM, JEOL JSM-6330F). The elemental distribution on the surface-modified separator was examined using energy dispersive X-ray spectroscopy (EDX). The thermal shrinkage of a pristine PE separator and surface-modified separators was measured in terms of their dimensional changes after being held at 130 °C for 30 min. In order to measure the ionic conductivity of PEDOT-*co*-PEG film, the film was soaked with liquid electrolyte and sandwiched between two stainless steel electrodes. AC impedance measurement was then performed to measure ionic conductivity using a Zahner Electrik IM6 impedance analyzer over the frequency range of 10 Hz–100 kHz with the amplitude of 10 mV. Charge and discharge cycling tests of the lithium-ion cells were conducted at a current density of 1.0 mA cm^{-2} (0.5C rate) over the voltage range from 3.0 to 4.5 V using battery test equipment (WBCS 3000, Wonatech). Surface characterization of the carbon negative electrodes in the cells after the repeated cycles was

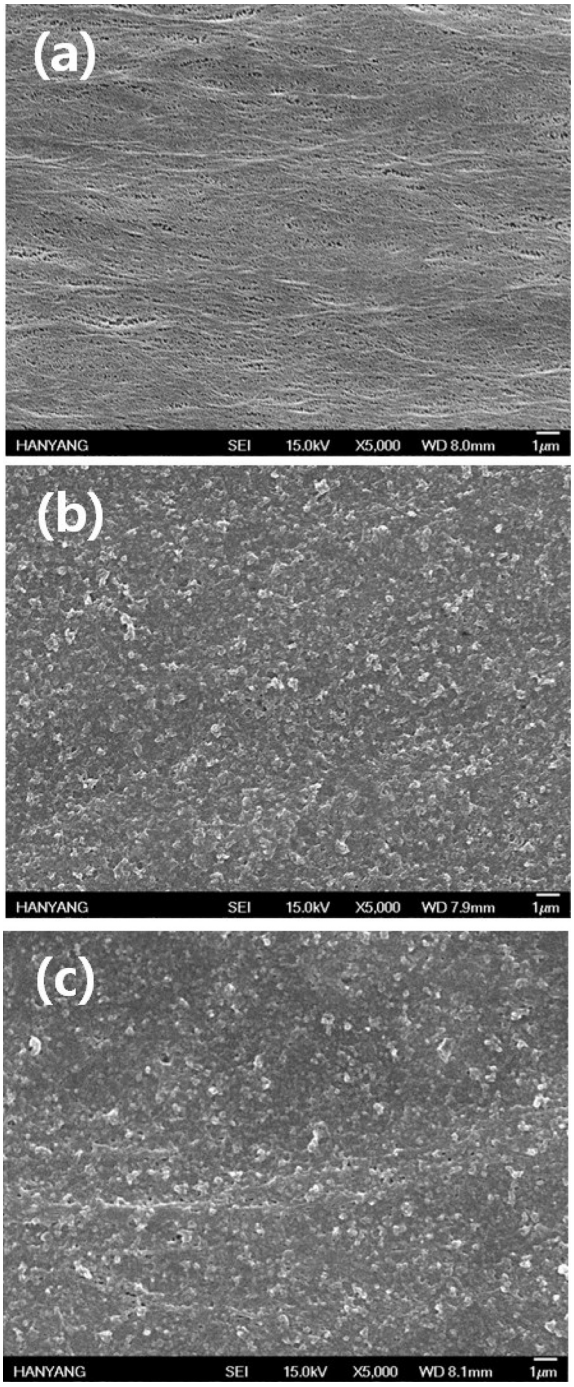

Fig. 1. FE-SEM images of different types of separators: (a) pristine PE separator, (b) surface-modified separator with PEDOT-*co*-PEG copolymer (SMS-1) and (c) surface-modified separator with PEDOT-*co*-PEG copolymer and AlF_3 particles (SMS-2).

conducted by X-ray photoelectron spectroscopy (XPS). The electrodes were washed several times with anhydrous dimethyl carbonate to remove residual electrolyte, followed by vacuum drying overnight at room temperature. They were transferred into an airtight container, mounted on an XPS sample holder and transferred to the XPS apparatus with minimal exposure to air. XPS measurements were conducted on a Thermo VG Scientific ESCA 2000 system using an Al Kα radiation source. HF content in the electrolyte was measured by an acid–base titration method after the cell was stored in a 55 °C oven for 3 days [24]. Methyl orange (Sigma–Aldrich) was used as an acid–base indicator.

3. Results and discussion

3.1. Characterization of the surface-modified separators

FE-SEM images of the surfaces of a pristine PE separator and surface-modified separators are presented in Fig. 1. The pristine PE separator exhibited a uniformly interconnected submicron pore structure. When the PEDOT-*co*-PEG copolymer and AlF_3 particles were coated on both sides of the PE separator, they covered the surface of the separator without agglomeration. The ionic conductivity of the PEDOT-*co*-PEG thin film soaked with the liquid electrolyte was 3.2×10^{-3} S cm^{-1}, indicating fast ion transport through the thin surface layer. The thin coating layer strongly adhered to the surface of the PE separator and its thickness was approximately 480 nm on each side. The durability of the coating layer was confirmed by washing the surface-modified separators (SMS-1 and SMS-2) several times with water or the liquid electrolyte used in this study. Neither the PEDOT-*co*-PEG copolymer nor the AlF_3 particles coated on the surface of the PE separator were removed after the washing procedure, indicating that the thin coating layers strongly adhered to both sides of the PE separator. The amounts of coated materials (PEDOT-*co*-PEG, or PEDOT-*co*-PEG and AlF_3) in SMS-1 and SMS-2 were 393.1 and 432.6 mg m^{-2}, respectively. Fig. 2 presents the EDX mapping images of various elements (C, O, Al and F) on the surface-modified separator with PEDOT-*co*-PEG and AlF_3 (SMS-2). Homogeneous distributions of carbon and oxygen in the PEDOT-*co*-PEG copolymer can be observed. It is also seen that the aluminum and fluorine elements arising from the AlF_3 particle are evenly distributed across the images, which indicates that the surface of the PE separator is uniformly coated with the PEDOT-*co*-PEG copolymer and AlF_3 particles.

The wettability of the separator plays an important role in battery performance because good wettability allows the separator to better retain the electrolyte solution, thereby facilitating fast ion transport between the two electrodes during charge and discharge cycling [5,6]. Photographs were taken of a pristine PE separator and surface-modified separators after dropping liquid electrolyte onto their surfaces. The pristine PE separator was not completely wetted and a liquid droplet was observed on its surface (Fig. 3(a)), whereas the surface-modified separators (SMS-1 in Fig. 3(b) and SMS-2 in Fig. 3(c)) were immediately wetted by the liquid electrolyte. Contact angles with water droplets were measured to compare the wettability of the separators; the results are shown in the lower part of Fig. 3. Clearly, the surface coating of PE separator with PEDOT-*co*-PEG copolymer greatly increased its wettability, producing a remarkable decrease in the contact angle from 103.0 to 61.5°, indicating that the surface-modified separator became much more hydrophilic due to the hydrophilic nature of the PEDOT-*co*-PEG coating layer. Moreover, the additional incorporation of AlF_3 into the coating layer further decreased the contact angle to 50.4°. This result is due to the fact that AlF_3 is highly hydrophilic and has good affinity with polar organic electrolytes [25].

To evaluate the heat resistance of different separators, we

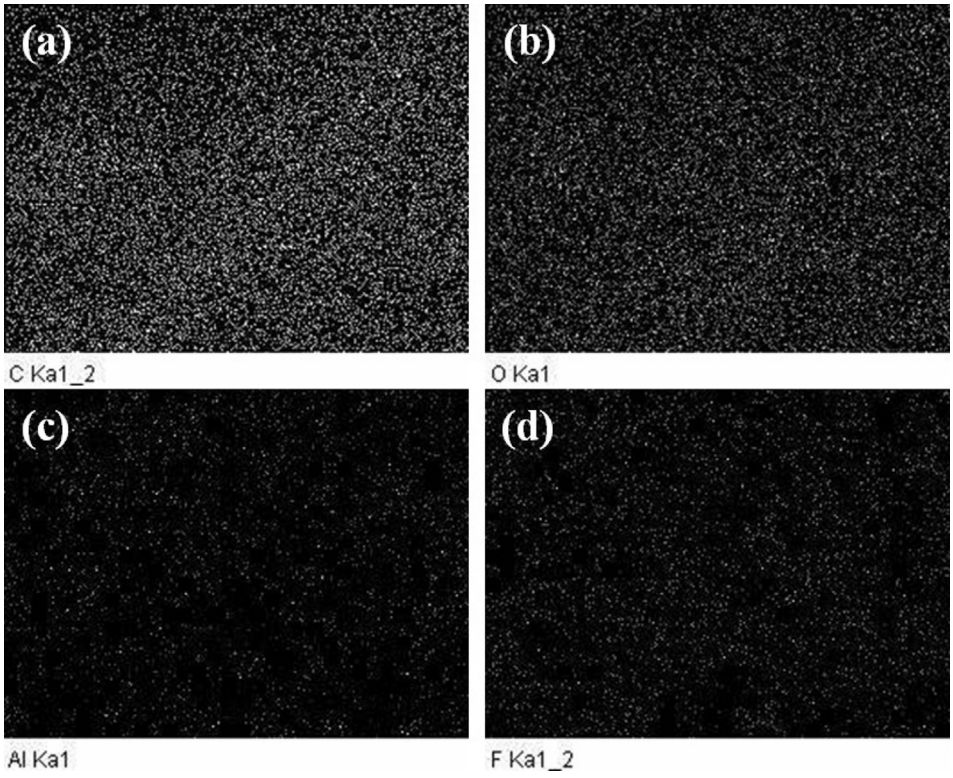

Fig. 2. EDX mapping images of (a) C, (b) O, (c) Al and (d) F on the surface-modified separator with PEDOT-*co*-PEG and AlF_3.

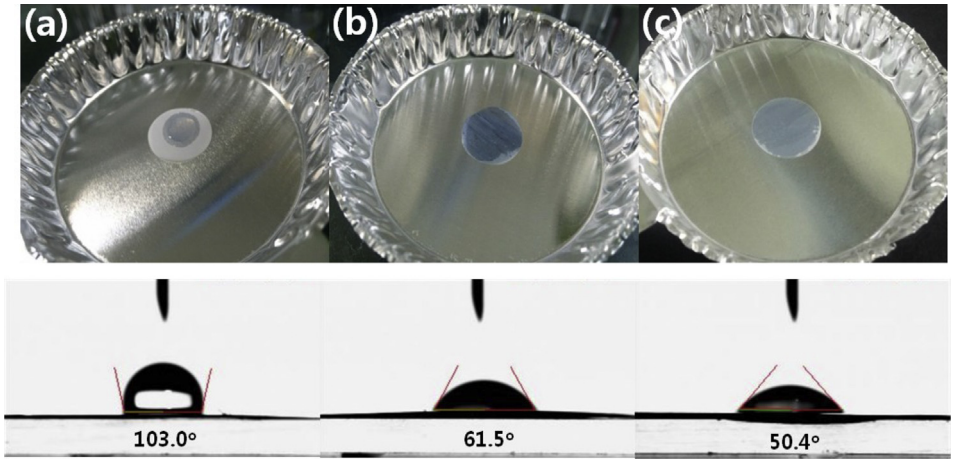

Fig. 3. Photographs of different separators after dropping liquid electrolyte onto their surfaces: (a) pristine PE, (b) SMS-1 and (c) SMS-2. Bottom: contact angle images of the corresponding separators.

measured their thermal shrinkage after holding them at 130 °C for 30 min; the results are shown in Fig. 4. As shown in figure, the pristine PE separator experienced a high degree of shrinkage (10.4%) during the high-temperature exposure. Because the manufacturing process of PE separators includes a drawing step, these separators easily shrink when exposed to high temperature [6], which may result in electric short circuits between negative electrode and positive electrode. However, the thermal shrinkage was remarkably reduced by coating both sides of the PE separator with PEDOT-*co*-PEG copolymer and AlF_3 particles. The PEDOT-*co*-PEG copolymer with good thermal stability strongly adhered to the PE separator. In addition, the inorganic AlF_3 particles could provide high heat resistance, helping to prevent thermal shrinkage of the separator at high temperature. As a result, the combined coating of the heat-resistant AlF_3 ceramic powders and thermally stable PEDOT-*co*-PEG copolymer onto both sides of the PE separator could prevent dimensional changes by thermal deformation at high temperature.

3.2. Evaluation of the cycling performance of lithium-ion cells

We evaluated the cycling performance of lithium-ion cells prepared with the surface-modified separators. The cells were initially subjected to a preconditioning cycle in the voltage range of 3.0–4.5 V at a constant current rate of 0.1C. After completing two cycles at the 0.1C rate, the cells were charged at a current density of 0.5C up to a cut-off voltage of 4.5 V. This was followed by a constant-voltage charge with declining current until a final current equal to 10% of the charging current was obtained. The cells were then discharged to a cut-off voltage of 3.0 V at the same current density. Fig. 5(a) shows the charge and discharge curves of the 1st, 10th, 20th, 50th, 100th and 200th cycles of a lithium-ion cell incorporating a separator coated with both PEDOT-*co*-PEG copolymer and AlF_3 particles (SMS-2). The cell had a relatively high initial discharge capacity of 182.2 mAh g^{-1} based on the active $LiNi_{1/3}Co_{1/3}Mn_{1/3}O_2$ material in the positive electrode. The discharge capacity of the cell declined to 143.7 mAh g^{-1} after 200 cycles. Fig. 5(b) shows the discharge capacities of lithium-ion cells incorporating the different separators as a function of cycle number. The initial discharge capacity of the cell was slightly increased by coating the PE separator with either the PEDOT-*co*-PEG copolymer or the combined coating of PEDOT-*co*-PEG copolymer and AlF_3 particles; this seemed to result from the improved ionic conductivity of the coated separators, due to the enhanced electrolyte uptake. The capacities of the cells incorporating the surface-modified separators were also retained better during repeated cycling. This result might be presumably due to the fact that the coatings could effectively improve the affinity between the electrolyte solution and the separator, which helped to prevent exudation of the electrolyte during cycling. In addition, the presence of AlF_3 can protect the $LiNi_{1/3}Co_{1/3}Mn_{1/3}O_2$ cathode particles from attack by HF in the electrolyte solution, as previously reported [19–21]. They reported that an AlF_3 coating on $LiCoO_2$ and $LiNi_{1/3}Co_{1/3}Mn_{1/3}O_2$ oxide particles improved both the capacity retention and the rate capability at high cut-off voltages, i.e., above 4.5 V.

To understand the effect of surface modification upon the performance of the cell, AC impedance spectra were collected for each type of cell before and after 200 cycles (Fig. 6). All the spectra exhibited two overlapping semicircles due to different contributions of interfacial resistances. The first semicircle in the higher frequency range can be attributed to the resistance due to Li^+ ion migration through the surface film on the electrodes (R_f), and the second semicircle in the middle to low frequency range arises from the charge transfer resistance at the electrode-electrolyte interface (R_{ct}) [26,27]. Before cycling (after two preconditioning cycles), the different types of cells had almost identical AC impedance spectra, except for small differences in the interfacial resistances (R_f and R_{ct}), indicating that the presence of the coating layers had little effect on the initial impedance of the cell. After charge and discharge cycling, the interfacial resistances increased for all of the cells. An increase in interfacial resistances is related to both the growth of resistive surface layer on the electrodes and the deterioration of the interfacial contacts at electrodes. The resistive layer formed on the electrode surface may hamper charge transport at the electrode and electrolyte interface, which increases the charge transfer resistance with the repeated cycles. It should be noted that the cells with surface-modified separators had lower interfacial resistances than the cell with the pristine PE separator. This result implies that the cells with surface-modified separators had more stable electrode–electrolyte interfaces, resulting in good capacity retention. Additionally, the electrolyte resistance that corresponds to the high-frequency intercept at the real axis was higher in the cell with the pristine PE separator, as shown in inset of Fig. 6(b). This result can be ascribed to loss of the electrolyte solution due to leakage, as well as to deleterious reactions between the electrolyte and the electrodes.

Fig. 7 compares the discharge capacities of the lithium-ion cells assembled with different separators, during experiments in which

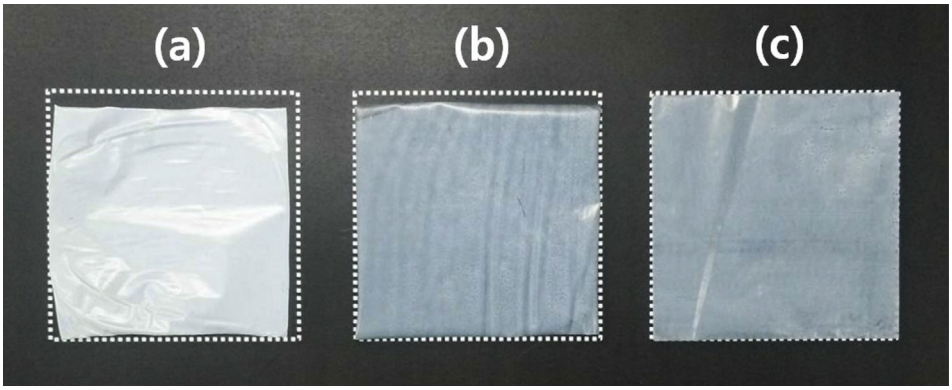

Fig. 4. Photographs of different separators after 130 °C exposure for 30 min: (a) pristine PE separator, (b) SMS-1 and (c) SMS-2.

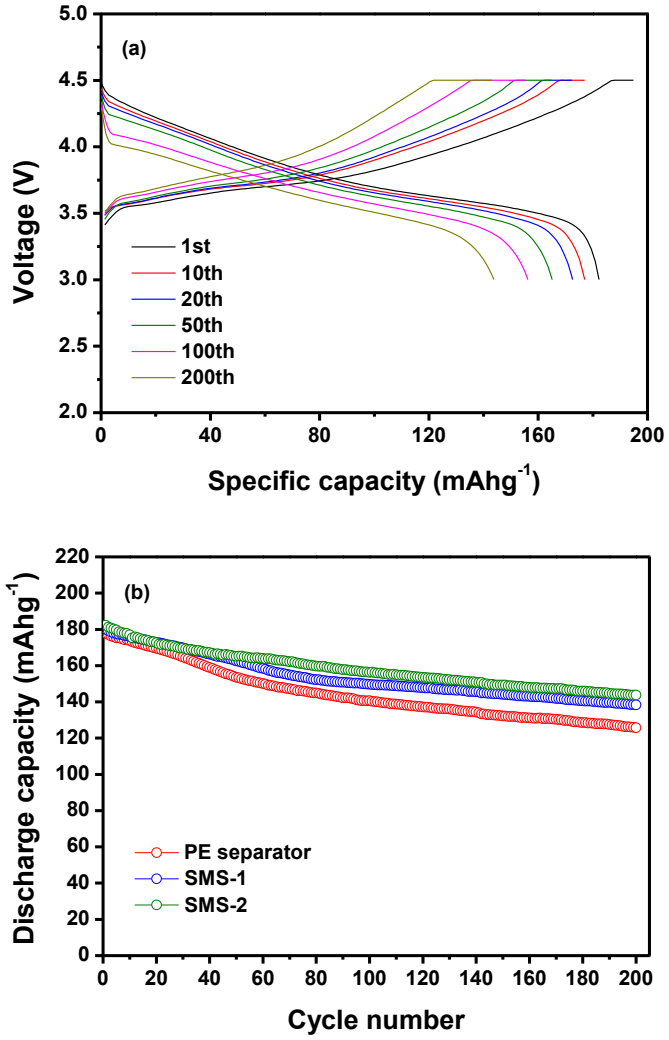

Fig. 5. (a) Charge and discharge curves of a lithium-ion cell assembled with SMS-2 (0.5C CC & CV charge, 0.5C CC discharge, cut-off voltage: 3.0–4.5 V, 25 °C), and (b) discharge capacities of lithium-ion cells prepared with the three different separators (0.5C CC & CV charge, 0.5C CC discharge, cut-off voltage: 3.0–4.5 V, 25 °C).

the C rates for the charge and discharge cycles were increased gradually every five cycles within the range of 0.1–5.0C. The discharge capacities gradually decreased as the C rate was increased, thereby demonstrating polarization. Clearly, the discharge capacities of the lithium-ion cell incorporating the separator coated with PEDOT-*co*-PEG and AlF_3 (SMS-2) were the highest for all C rates tested. As shown in Fig. 6, the ionic resistance was lowest in the cell including the SMS-2 separator, thereby reducing the concentration polarization of the electrolyte during

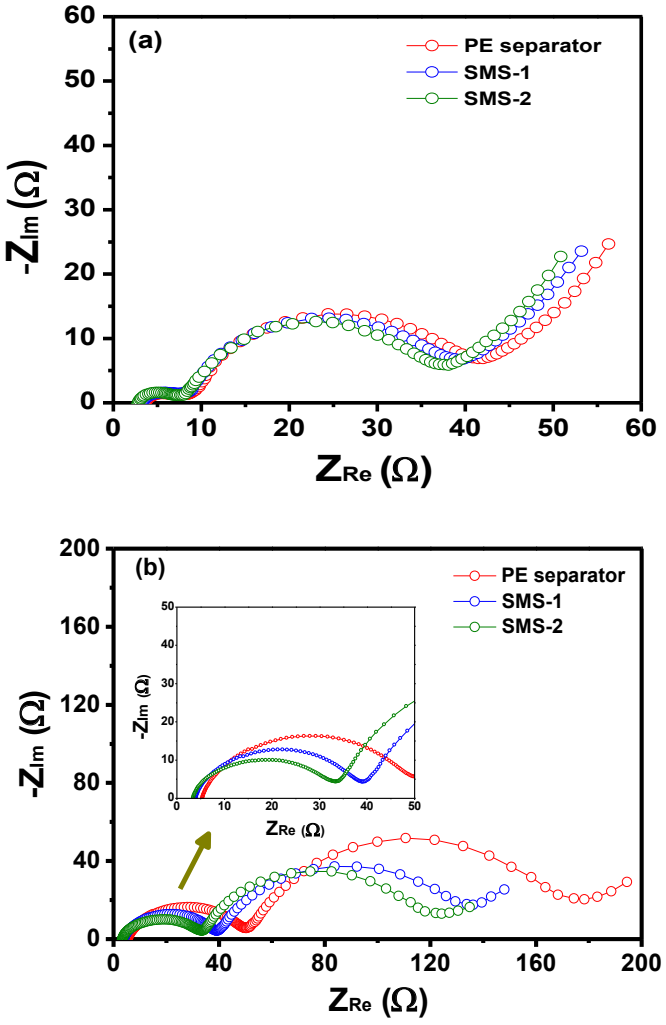

Fig. 6. AC impedance spectra of lithium-ion cells incorporating the three different types of separators, measured (a) before and (b) after 200 cycles. The inset shown in (b) presents a close-up view in the higher frequency range.

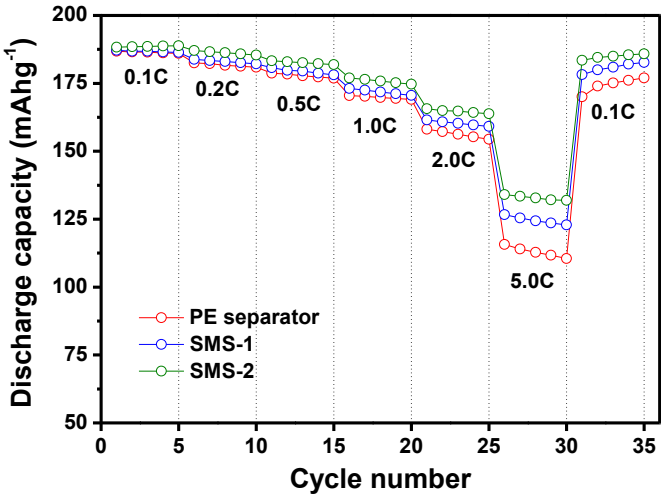

Fig. 7. Discharge capacities of lithium-ion cells assembled with different separators at 25 °C, as a function of C rate. The C rate was increased from 0.1 to 5.0C after every 5 cycles.

cycling. The polymer layer on both sides of the PE separator was also expected to assist in retaining the adhesion of the separator to the electrodes after soaking in the electrolyte solution, resulting in the favorable interfacial charge transport between the electrodes and electrolyte in the cell.

Fig. 8 shows the discharge capacities of the lithium-ion cells assembled with different separators as a function of the cycle number, obtained at 55 °C and 0.5C rate. The cells delivered initial discharge capacities ranging from 186.9 to 192.9 mAh g^{-1}, which were higher than those obtained at 25 °C. As can be seen in Fig. 8, the capacity retention was remarkably improved by incorporating surface-modified separators. It is well known that layered $LiNi_xCo_yMn_{1-x-y}O_2$ materials experience gradual capacity fading at high temperatures due to structural and interfacial instabilities as well as dissolution of transition metals from the active cathode material by HF attack [28,29]. It is thus plausible that the differences in high-temperature cycling stability of the different cell types are closely related to the content of HF in the electrolyte. HF is known to be generated by thermal decomposition and hydrolysis of $LiPF_6$ by trace moisture in the electrolyte solution [30,31]. We measured HF content in the cells with different separators after storing the cells at 55 °C for 3 days. After this storage, the HF contents were 161, 96 and 86 ppm in the cells with the PE separator, SMS-1 and SMS-2, respectively. PEG in the PEDOT-*co*-PEG

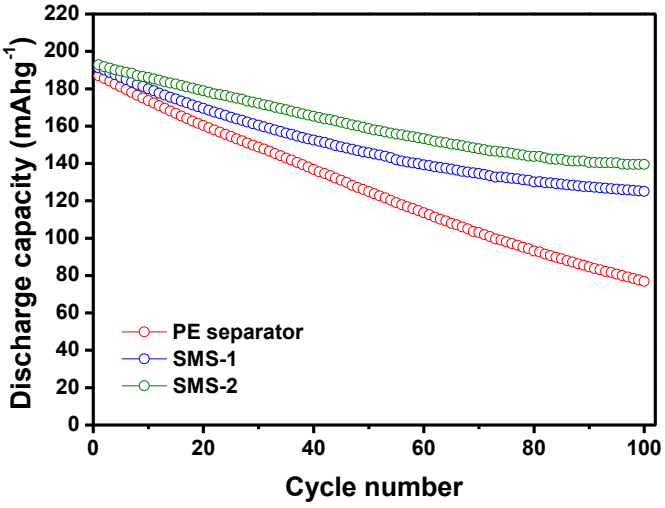

Fig. 8. Discharge capacities at 55 °C versus cycle number for lithium-ion cells incorporating the three different types of separators (0.5C CC & CV charge, 0.5C CC discharge, cut-off voltage: 3.0–4.5 V).

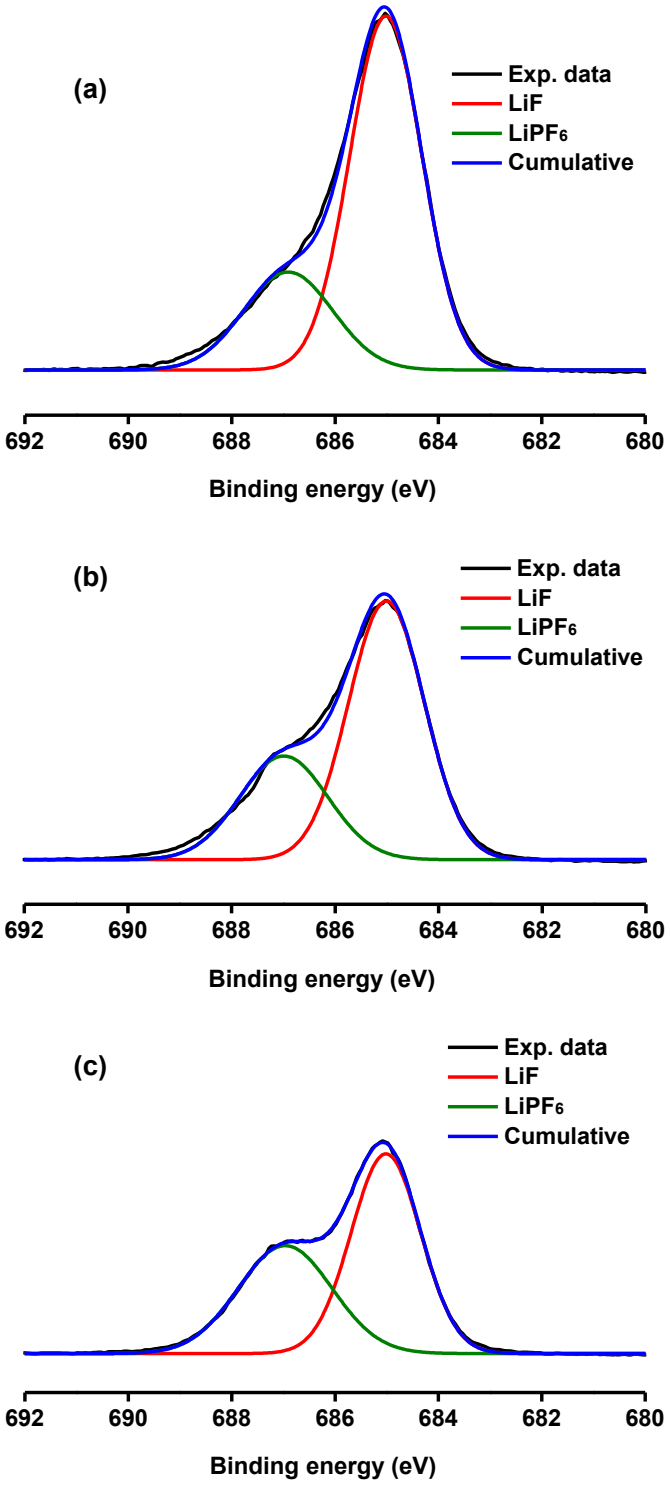

Fig. 9. XPS spectra (F 1s) of the surfaces of carbon negative electrodes in cells incorporating the three different separators: (a) pristine PE, (b) SMS-1 and (c) SMS-2. All spectra were obtained after 100 cycles at 55 °C.

copolymer is a Lewis base, and thus could effectively complex with thermally decomposed PF_5 that is a Lewis acid [32], thereby preventing its hydrolysis to produce HF. Li et al. reported that the addition of Lewis basic additives could stabilize organic electrolytes against thermal decomposition initiated by Lewis acids [33]. Consequently, the use of surface-modified separators containing PEDOT-*co*-PEG reduced the HF content and thus suppressed the dissolution of transition metals from the active $LiNi_{1/3}Co_{1/3}Mn_{1/3}O_2$ material at elevated temperatures. As a result, the cells assembled with surface-modified separators exhibit more stable cycling behavior at 55 °C. In the case of a cell with a pristine PE separator, the dissolution of transition metals by HF attack may cause a rapid increase in the interfacial resistance, thereby accelerating the capacity loss as cycling progresses at elevated temperatures.

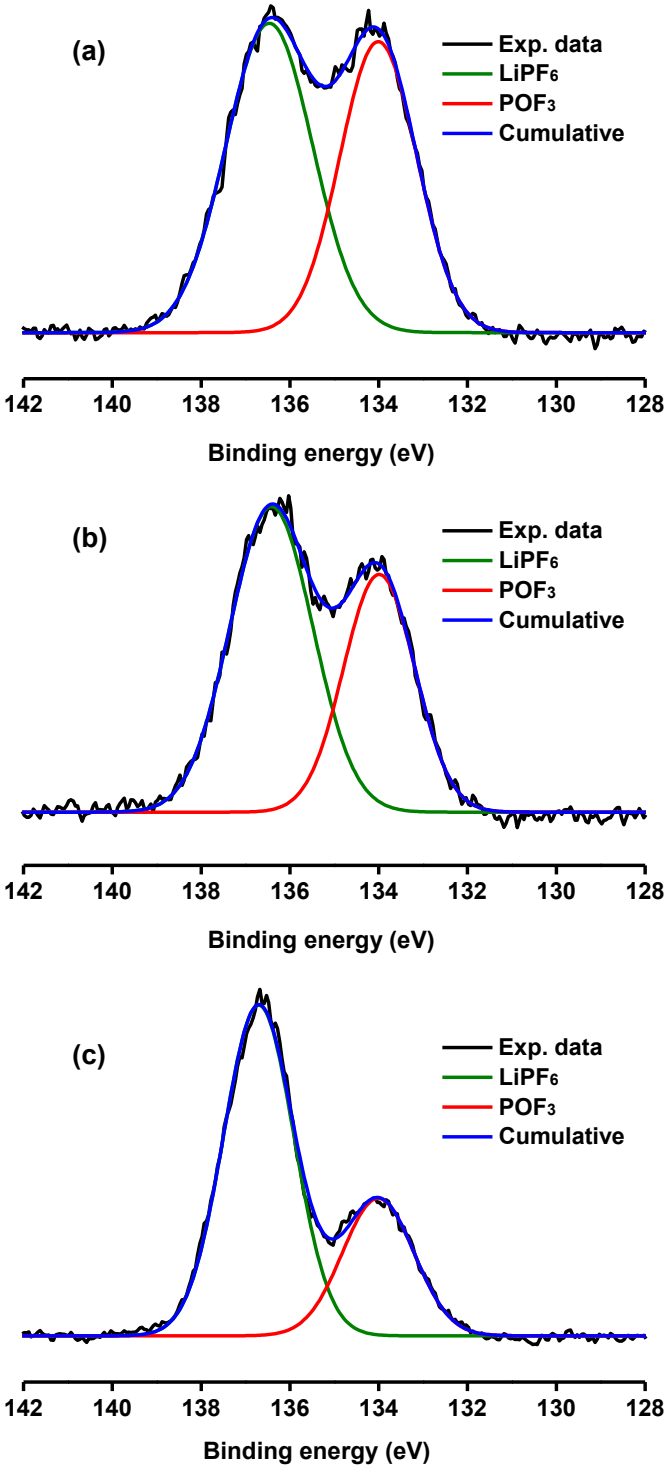

Fig. 10. XPS spectra (P 1s) of the surfaces of carbon negative electrodes in cells incorporating the three different separators: (a) pristine PE, (b) SMS-1 and (c) SMS-2. All spectra were obtained after 100 cycles at 55 °C.

3.3. XPS analysis of carbon electrodes

The surfaces of the carbon negative electrodes in cells incorporating different separators were analyzed by means of XPS after 100 cycles at 55 °C, and the results are shown in Figs. 9 and 10. The highly resistive LiF, observed at 685.0 eV for F 1s [34,35], was most abundant on the electrode surface of the cell that incorporated a pristine PE separator (Fig. 9). In lithium-ion cells, LiF is produced by the thermal decomposition of $LiPF_6$ salt on the electrode surface [30]. It is an insulating material for both electrons and Li^+ ions, and thus LiF that forms on the surface of the electrode may hamper the charge transfer reaction between the electrode and the electrolyte, thereby increasing the charge transfer resistance. The intensity of the XPS peak corresponding to POF_3, which is generated by the decomposition of $LiPF_6$, was also strongest on the carbon electrode of the cell with pristine PE separator (Fig. 10). The atomic compositions on the surface of carbon electrodes provided an additional support. The oxygen concentration was higher in the carbon electrode of the cell with pristine PE separator, which is well consistent with the deposition of more electrolyte decomposition product (POF_3). These results suggest that the coating of PEDOT-*co*-PEG and AlF_3 onto PE separators was very effective in suppressing electrolyte decomposition at high temperature, which is consistent with the cycling results presented in Fig. 8.

The results presented herein demonstrated that cells assembled with surface-modified separators exhibited superior cycling performance compared to cells prepared with pristine PE separators, both at ambient temperatures and at elevated temperature.

4. Conclusions

Surface-modified separators were prepared by coating PEDOT-*co*-PEG copolymer and AlF_3 particles onto both sides of PE separator. The thin coating layers formed on the PE separators significantly improved their liquid electrolyte wettability and their thermal stability. The lithium-ion cells assembled with the surface-modified separators exhibited better cycling performance than a cell with a pristine PE separator. Thus, it is expected that the surface-modified separators prepared in this study will be useful as separators for rechargeable lithium-ion batteries, which require good cycling stability, high energy density and enhanced thermal safety.

Acknowledgments

This work was supported by the Basic Science Research Program of the National Research Foundation of Korea, funded by the Ministry of Science, ICT and Future Planning (2014R1A2A2A01002154), and by a grant from the Human Resources Development Program of KETEP, funded by the Ministry of Trade, Industry and Energy, Korea (No. 20124010203290).

References

[1] M. Winter, R.J. Brodd, Chem. Rev. 104 (2004) 4245–4269.
[2] A.S. Arico, P. Bruce, B. Scrosati, J.-M. Tarascon, W.V. Schalkwijk, Nat. Mater. 4 (2005) 366–377.

[3] B. Dunn, H. Kamath, J.-M. Tarascon, Science 334 (2011) 928–935.
[4] V. Etacheri, R. Marom, R. Elazari, G. Salitra, D. Aurbach, Energy Environ. Sci. 4 (2011) 3243–3262.
[5] P. Arora, Z. Zhang, Chem. Rev. 104 (2004) 4419–4462.
[6] S.S. Zhang, J. Power Sources 164 (2007) 351–364.
[7] G. Venugopal, J. Moore, J. Howard, S. Pendalwar, J. Power Sources 77 (1999) 34–41.
[8] I. Uchida, H. Ishikawa, M. Mohamedi, M. Umeda, J. Power Sources 119–121 (2003) 821–825.
[9] M.S. Wu, P.C.J. Chiang, J.C. Lin, Y.S. Jan, Electrochim. Acta 49 (2004) 1803–1812.
[10] J. Saunier, F. Alloin, J.Y. Sanchez, G. Caillon, J. Power Sources 119–121 (2003) 454–459.
[11] Y.M. Lee, J.W. Kim, N.S. Choi, J.A. Lee, W.H. Seol, J.K. Park, J. Power Sources 139 (2005) 235–241.
[12] J.A. Choi, S.H. Kim, D.W. Kim, J. Power Sources 195 (2010) 6192–6196.
[13] M.H. Ryou, Y.M. Lee, J.K. Park, J.W. Choi, Adv. Mater. 23 (2011) 3066–3070.
[14] H.S. Jeong, S.Y. Lee, J. Power Sources 196 (2011) 6716–6722.
[15] X. Huang, J. Power Sources 196 (2011) 8125–8128.
[16] W.K. Shin, D.W. Kim, J. Power Sources 226 (2013) 54–60.
[17] I.S. Kang, Y.S. Lee, D.W. Kim, J. Electrochem. Soc. 161 (2014) A53–A57.
[18] S.H. Ju, I.S. Kang, Y.S. Lee, W.K. Shin, S. Kim, K. Shin, D.W. Kim, ACS Appl. Mater. Interfaces 6 (2014) 2546–2552.
[19] Y.K. Sun, S.W. Choi, S.W. Lee, C.S. Yoon, K. Amine, J. Electrochem. Soc. 154 (2007) A168–A172.
[20] H.B. Kim, B.C. Park, S.T. Myung, K. Amine, J. Prakash, Y.K. Sun, J. Power Sources 179 (2008) 347–350.
[21] Y.K. Sun, M.J. Lee, C.S. Yoon, J. Hassoun, K. Amine, B. Scrosati, Adv. Mater. 24 (2012) 1192–1196.
[22] S.M. Eo, E. Cha, D.W. Kim, J. Power Sources 189 (2009) 766–770.
[23] F. Ding, W. Xu, D. Choi, W. Wang, X. Li, M.H. Engelhard, X. Chen, Z. Yang, J.-G. Zhang, J. Mater. Chem. 22 (2012) 12745–12751.
[24] Y.K. Sun, K.J. Hong, J. Prakash, K. Amine, Electrochem. Commun. 4 (2002) 344–348.
[25] C. Alonso, A. Morato, F. Medina, F. Guirado, Y. Cesteros, P. Salagre, J.E. Sueiras, R. Terrado, A. Giralt, Chem. Mater. 12 (2000) 1148–1155.
[26] Y. Bai, X. Wang, X. Zhang, H. Shu, X. Yang, B. Hu, Q. Wei, H. Wu, Y. Song, Electrochim. Acta 109 (2013) 355–364.
[27] T. Liu, A. Garsuch, F. Chesneau, B.L. Lucht, J. Power Sources 269 (2014) 920–926.
[28] G.G. Amatucci, J.M. Tarascon, L.C. Klein, Solid State Ionics 83 (1996) 167–173.
[29] S.U. Woo, B.C. Park, C.S. Yoon, S.T. Myung, J. Prakash, Y.K. Sun, J. Electrochem. Soc. 154 (2007) A649–A655.
[30] H. Yang, G.V. Zhuang, P.N. Ross Jr., J. Power Sources 161 (2006) 573–579.
[31] E. Zinigrad, L. Larush-Asraf, J.S. Gnanaraj, M. Sprecher, D. Aurbach, Thermochim. Acta 438 (2005) 184–191.
[32] A.M. Stephan, K.S. Nahm, Polymer 47 (2006) 5952–5964.
[33] W. Li, C. Campion, B.L. Lucht, B. Ravdel, J. DiCarlo, K.M. Abraham, J. Electrochem. Soc. 152 (2005) A1361–A1365.
[34] D. Aurbach, K. Gamolsky, B. Markovsky, Y. Gofer, M. Schmidt, U. Heider, Electrochim. Acta 47 (2002) 1423–1439.
[35] D. Aurbach, I. Weissman, A. Schechter, Langmuir 12 (1996) 3991–4007.